Eur. Phys. J. B **48**, 65–70 (2005)
DOI: 10.1140/epjb/e2005-00384-y

THE EUROPEAN PHYSICAL JOURNAL B

Semiconductor concentric double rings in a magnetic field

J. Planelles[1,a] and J.I. Climente[1,2]

[1] Departament de Ciències Experimentals, UJI, Box 224, 12080 Castelló, Spain
[2] CNR-INFM-S3, Università degli Studi di Modena e Reggio Emilia, via Campi 213/A, 41100 Modena, Italy

Received 4 August 2005 / Received in final form 20 October 2005
Published online 9 December 2005 –

Abstract. We report a theoretical study on the magnetooptical properties of recently synthesized concentric quantum double rings, as a function of the inner-outer ring coupling. The transition from a single to a double ring, as it is reflected in the the changes of the Aharonov-Bohm oscillation periods of the energy levels, is shown. It is found that, even when the system can be described as a single quantum ring with a small cleft, the electron energy levels show two different Aharonov-Bohm oscillation periods, which indicate that the carriers are localized in either the inner or the outer ring. For most distances between the rings, the electron and hole energy levels show almost identical Aharonov-Bohm oscillation periods. However, there is a short distances range in which they do not localize in the same ring, showing very different periods. In this region, the exciton ground state becomes dark.

PACS. 73.21.-b Electron states and collective excitations in multilayers, quantum wells, mesoscopic, and nanoscale systems – 75.75.+a Magnetic properties of nanostructures

1 Introduction

Semiconductor quantum dots (QDs) are zero-dimensional systems which are the core of novel nanotechnological devices. This has induced their intensive study for the last two decades [1,2]. Ever since these structures were first synthesized, there has been a continuous effort to tailor their size, shape and composition, since these parameters control the electronic states and physical properties. Thus, small spherical QDs, made of one or more concentric shells of different semiconductor materials, have been synthesized using wet chemistry methods [3,4]. QDs with geometries including pyramids, truncated pyramids and lenses have been obtained using self-assembly growth techniques [2]. More recently, ring-shaped QDs, often referred to as quantum rings (QRs), have also been synthesized by self-assembly techniques [5,6]. These systems have attracted considerable attention because they combine the excellent optical properties of self-assembled nanostructures [7] with the singular magnetic properties [8] originated by their non-simply connected topology, which gives rise to the Aharonov-Bohm (AB) effect [9]. Last January, experimental self-assembly of concentric $GaAs/Al_xGa_{1-x}As$ quantum double rings was for the first time reported [10]. Atomic force microscope (AFM) images revealed that these structures have clear rotational symmetry, with two concentric rings about 4 nm high and average diameters at the point of maximum height of 45 nm and 100 nm, for the inner and outer ring respectively. Interestingly enough, it was indicated that, by controlling the As flux intensity in the fabrication process, the outer diameter can be controlled whereas the inner one remains almost unchanged. Experimental photoluminescence data reported was well interpreted by employing the effective mass approximation [10].

In the present paper, we carry out a theoretical study on the magnetooptical properties of these novel quantum rings. We calculate the electron and hole energy levels, as well as the corresponding far-infrared (FIR) absorption spectra, for a set of double rings with fixed inner ring radius but different outer ring radii.

2 Theoretical considerations

We use a three-dimensional, one-band effective mass Hamiltonian for both electrons and holes, including a magnetic field perpendicular to the ring plane. In atomic units and cylindrical coordinates, the Hamiltonian reads

$$\mathcal{H} = -\frac{1}{2}\nabla\left(\frac{1}{m_q^*(\rho,z)}\,\nabla\right)+\frac{(B\,\rho)^2}{8m_q^*(\rho,z)}+\frac{B\,m}{2m_q^*(\rho,z)}+V_c(\rho,z), \tag{1}$$

where $m = 0, \pm1, \pm2,...$ is the quantum number of the angular momentum projection onto the magnetic field (B) axis, n is the main quantum number, $V_c(\rho,z)$ is the finite confinement potential corresponding to the geometries shown in the insets of Figures 1 and 2, and $m_q^*(\rho,z)$ stands for the position-dependent mass,

[a] e-mail: planelle@exp.uji.es

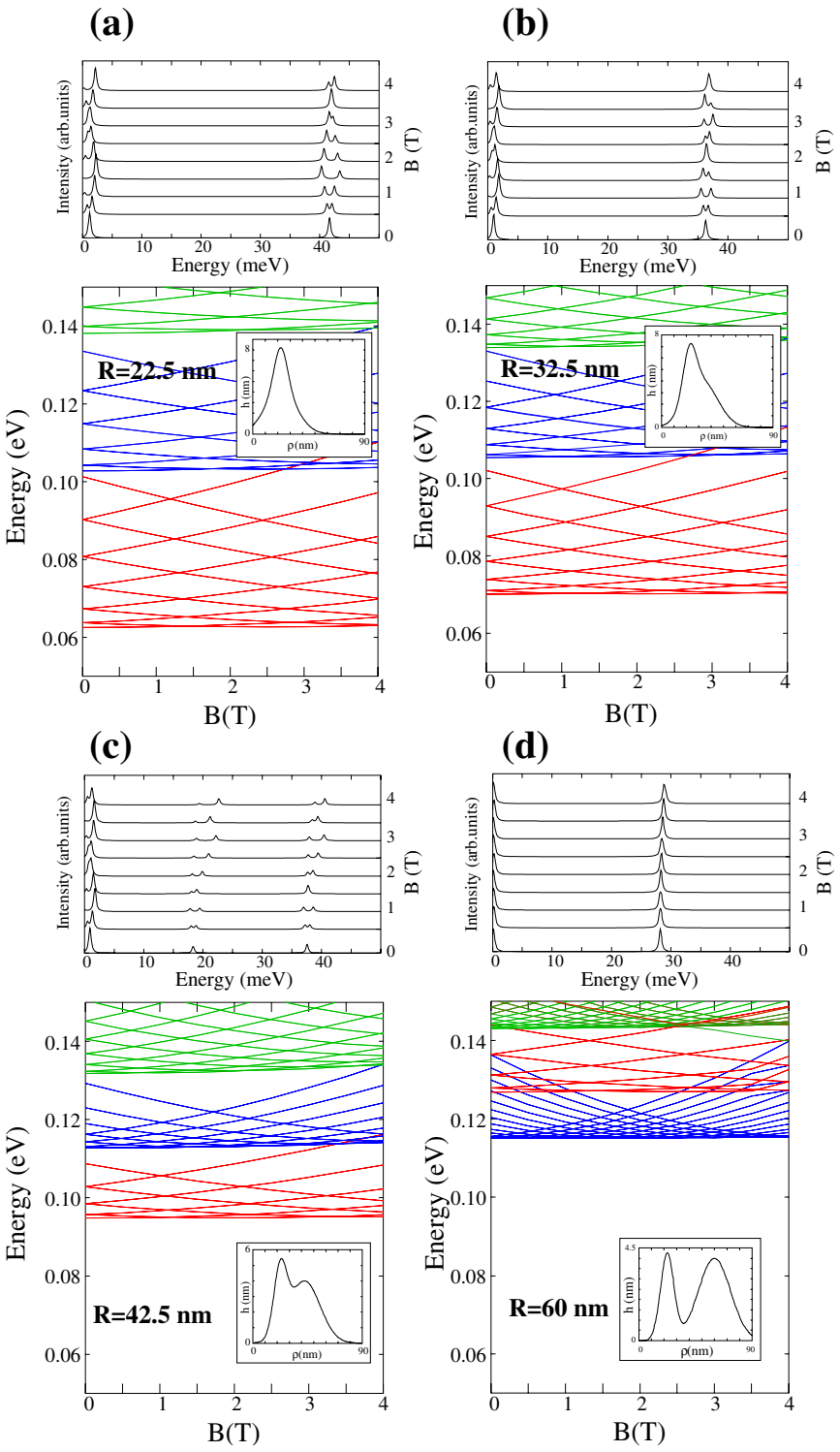

Fig. 1. FIR spectra (upper part) and energy levels (lower part) vs. magnetic field of one electron in quantum double rings whose cross-section profile are shown in the insets. The radius of the inner ring is 22.5 nm. The outer radii values are (a) 22.5, (b) 32.5, (c) 42.5, and (d) 60 nm. For sake of clearness only the low energy states of $r\ n = 0, 1, 2$, are displayed. Red lines represent the lowest state with maximum charge density in the inner ring. Blue and green lines, those of maxima in the outer ring.

with q=e for electrons and q=h for holes. It should be underlined that V_c must be a step-like, finite confinement potential in order to achieve a realistic description of the effect of the inner hole and the magnetic field penetration into the ring region [11,12]. The convenience of using a three-dimensional model, which takes the vertical confinement explicitly into account, is endorsed by the strong sensitivity of the energy spectrum to the depth of the valley separating the inner and outer rings, as we shall discuss later. The FIR absorption spectra are calculated within the electronic dipole approximation [13]. We assume T=0 K, so that only the ground state is occupied, and represent the transition probabilities by Lorentzian curves of half-width Γ=0.5 meV. A configuration interaction procedure is used to calculate the two-body eigenstates and eigenenergies [13].

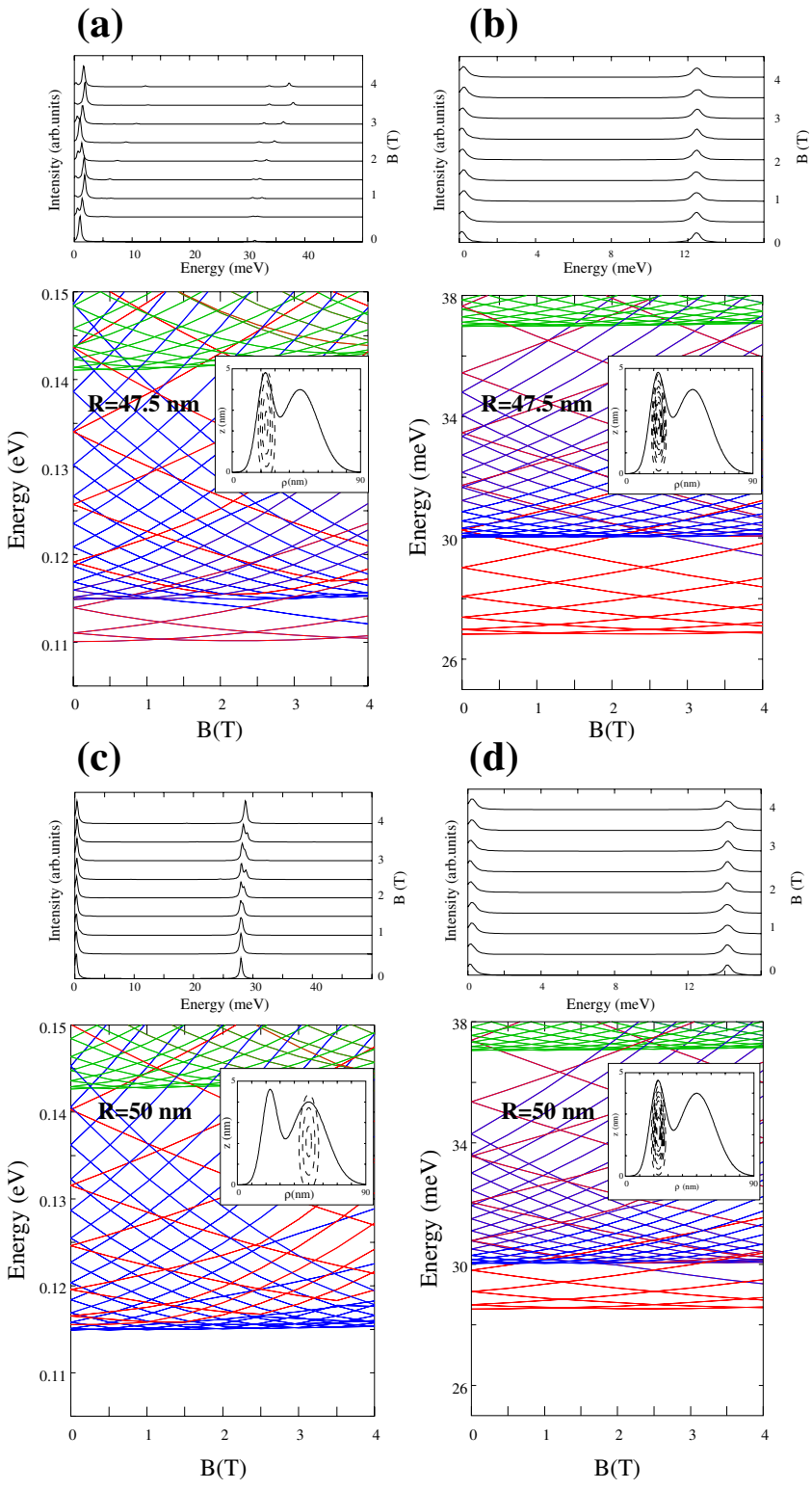

Fig. 2. FIR spectra (upper part) and energy levels (lower part) vs. magnetic field of one electron ((a) and (c)) and one hole ((b) and (d)) in quantum double rings. The inner ring radius is 22.5 nm and the outer ring one 47.5 ((a), (b)) and 50 nm ((c), (d)). In the insets, the quantum double ring cross-section profile (solid lines) and charge density distribution contours of the ground state at $B = 0$ T (dashed lines) are shown.

3 Results and discussion

We investigate self-assembled GaAs quantum double rings embedded in a $Al_{0.3}Ga_{0.7}As$ matrix. According to AFM images [10], the double ring is well described as the superimposition of two concentric rings with Gaussian-like cross-section profile. The inner ring is thinner and slightly taller than the outer one. Thus, in our calculations we take the inner/outer ring height as 4.2 nm and 4 nm, respectively, and the corresponding half-widths as 12.5 nm and 30 nm. The radius of the inner ring (from the origin to the top of the Gaussian-like cross-section) is fixed at 22.5 nm, while that of outer ring ranges from 22.5 nm (both rings being superimposed) up to 60 nm.

The same material parameters as in reference [10] are used here, namely $m_e^*(\mathrm{GaAs}) = 0.067$, $m_h^*(\mathrm{GaAs}) = 0.51$, $m_e^*(\mathrm{Al_{0.3}Ga_{0.7}As}) = 0.093$, $m_h^*(\mathrm{Al_{0.3}Ga_{0.7}As}) = 0.57$, CB/VB band-offsets 262 meV and 195 meV, respectively. Equation (1) is integrated numerically by employing finite differences in a two-dimensional grid (ρ, z).

Figure 1 shows the energy levels (bottom panel) and FIR absorption (top panel) vs. the magnetic field of one electron in four quantum double rings with different outer ring radii R. When $R = 22.5$ nm, the inner and outer rings are superimposed. Thus, the energy levels describe the expected Aharonov-Bohm oscillations, which are quasi-periodical, the ground state period being about 2 T. For $R = 42.5$ nm, when the cross-section profile looks like a single ring with a small cleft (see inset in Fig. 1c), the energy levels already show two clearly different oscillation periods: about 2 T for the $n = 0$ ground state (similar to the single ring case) and half this period for the $n = 1$ low-lying excited levels. This means that the electronic density of the ground state localizes mostly in the inner ring, while that of the excited states already localizes in the (slightly less voluminous) outer ring. The same picture holds for $42.5 < R < 50$ nm. Moreover, we can see that as R increases the energy levels become destabilized, the energy of the $n = 0$ states being far more sensitive to R than those of $n = 1$. This is because the area of the double ring cross-section is fixed for all values of R and the outer ring has significantly larger half-width than the inner one. Therefore, as R increases the room in the inner ring is severely reduced (see insets in Figs. 1 and 2). For large enough values of R, the ground state is already localized in the outer ring (Fig. 1d). We have also investigated whether a strong magnetic field is able to induce a crossover of the ground state charge density from the outer to the inner ring. However, the results suggest that, for quantum double rings like those synthesized in reference [10], the magnetic field cannot compete against the strong vertical confinement.

At this point it is interesting to underline some significative differences between our single-electron results and those reported in a parallel work by other authors [14]. In that work, the electron localization in the inner or outer ring of a concentric QR structure is found to be dependent on the angular momentum through the centrifugal potential in the Hamiltonian. In addition, when the rings are weakly coupled the magnetic field is able to transfer the charge density from the outer to the inner ring. This is in contrast with the picture we have described above (rather closer to early predictions by Fuster et al. [15]), where the electron localization is essentially determined by the spatial confinement and only the presence of radial nodes n may lead to severe changes in the charge distribution, so that the energy levels of two concentric QRs in a magnetic field are roughly the superposition of each ring's levels. Most likely these differences are due to the soft parabolic confinement potential employed in the theoretical model of reference [14]. Since our confinement potential has been fitted from reference [10] concentric QRs profile and band-offset parameters, taking into account the details of the strong vertical confinement, our results should provide a more accurate description of the experimentally synthesized nanostructures.

As for the FIR absorption, Figure 1a shows a typical single QR spectrum: two sets of absorption peaks, a low-energy one connected with $\Delta n = 0$ transitions and a high-energy one connected with $\Delta n = 1$ transitions. The external magnetic field splits these peaks into $\Delta m = \pm 1$ branches with oscillating energies [13]. When R starts increasing (Figs. 1a to 1c), the $\Delta n = 1$ transition changes progressively: its energy and intensity decrease gradually because the $n = 1$ state localizes in the expanding outer ring whereas the ground state remains in the inner ring. However, for $R > 50$ nm the $\Delta n = 1$ transition suddenly exhibits an abrupt change, as it shows a peak of similar intensity to that of the $\Delta n = 0$ transition at about 28 meV (see Fig. 2c). This is because the ground state density has crossed from the inner to the outer ring. A similar spectrum is obtained for larger values of R (see Fig. 1d). Hole states calculations give very similar results to those we have discussed for electrons here.

Figure 2 shows the energy levels and FIR absorption spectra vs. magnetic field corresponding to one electron/hole in a quantum double ring with $R = 47.5$ nm (Figs. 2a/2b) and $R = 50$ nm (Figs. 2c/2d). By comparing the energy oscillation periods of electrons and holes, no remarkable difference can be seen. This is somehow surprising, because when both particles are confined in the same ring, their very different masses and band-offset potentials are known to give different oscillation periods (see e.g. Fig. 5 in Ref. [16])[1]. Here the situation is different due to the particular Gaussian-like cross-section of the double ring (with pronounced tops at two given radii), which makes the density distribution of electrons and holes very similar, mainly localized near the region where the Gaussian profile has a top. As a consequence, the AB oscillation periods of both types of carriers are also very similar. Nonetheless, it is possible to find a (short) range of outer ring radii where electrons and holes are localized in different rings (see insets in Figs. 2c and 2d), forming a type-II QR. This should yield a dramatic decrease in the photoluminescence emission intensity, due to the reduced overlap between electrons and holes. In addition, in such a system electrons and holes have very different AB oscillation periods (see Figs. 2c and 2d). Consequently, the selection rule for the exciton to disappear emitting a photon ($M = m_e + m_h = 0$) only holds in the extremely short range 0–0.3 T. For stronger magnetic fields, the photoluminescence emission is completely forbidden[2].

[1] Different oscillation periods are related to different magnetic flux crossing the system. Since the magnetic field is the same for both electrons and holes, it follows that differences should come from different mean radii of the charge distributions. In general, different masses and confining band offsets yield different density mean radius for an electron and a hole confined in the same region of the space.

[2] It is interesting to note that here this phenomenon, known as the optical AB effect [17], is predicted to take place at much weaker magnetic fields than in typical InAs self-assembled QRs [16].

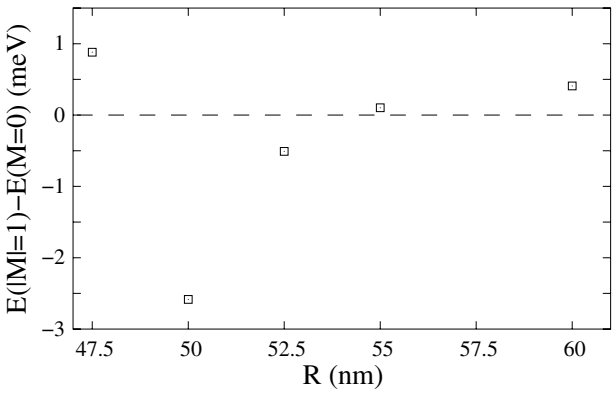

Fig. 3. Energy difference between the lowest $|M| = 1$ and $M = 0$ exciton states at $B = 0$ T vs. the radius of the outer ring.

We have explored with more detail, at $B = 0$ T, the radii range which includes the region where electron and hole localize in different rings. To this end we incorporate the electron-hole attraction and carry out CI calculations. The obtained results indicate that, even in the absence of an external magnetic field, the exciton is dark in this region ($M \neq 0$). Thus, we find the exciton ground state bright ($M = 0$) at $R = 47.5$ nm and 60.0 nm, and dark ($|M| = 1$) at $R = 50$ nm. The CI expansions show that the one-particle picture is still valid when the ground state of both particles localize them in the inner ring ($R \leq 47.5$). In the region in which the one-particle ground states of electron and hole localize in different rings, the configurations with highest weights included in the multiconfigurational exciton ground state confine, though, electron and hole in the same (inner) ring but the ground state angular momentum results to be $|M| = 1$, i.e., it is a dark exciton. Indeed, at this geometry the lowest bright state is the second excited one. When both particles localize their ground states in the outer ring, the exciton is bright again. However, the CI expansion does not show a single dominant configuration but several configurations with comparable weights. This is due to the fact that the low-lying part of the energy spectra of particles located in the outer ring is quite dense (see Figs. 1 and 2). We summarize the exitonic results in Figure 3 in which we display the energy difference between the lowest $M = 0$ and $|M| = 1$ exitonic states at $B = 0$ T vs. R and show the dark exciton region found.

4 Conclusions

In summary, we have studied the energy structure and FIR absorption spectra of concentric quantum double rings as a function of the coupling between the inner and outer rings. It has been shown that, even in the presence of a significant coupling, the oscillations of the energy levels vs. the magnetic field show two very different periods, which means that the charge density of the states is mostly localized in either the inner or the outer ring. Since the overlap between states in different rings is small, only transitions between states localized in the same ring are strong. Therefore, the quantum double ring FIR absorption looks similar to that of a single QR. The ground state charge density crossover from the inner to the outer ring at a given value of the outer ring radius produces an abrupt change in the FIR spectrum, which may be useful to determine spectroscopically the electron localization in these nanostructures. Due to the particular Gaussian-like cross-section of quantum double rings, the charge density of electrons and holes is mainly localized under the top of one of the concentric rings, so that their AB oscillation periods are very similar. However it is possible to find a (short) range of outer ring radii where electrons and holes localize in different rings and thus have very different oscillation periods. In such a case, the ground exciton becomes dark and the photoluminescence emission should then be suppressed.

We thank M. Pi for helpful comments. Financial support from MEC-DGI project CTQ2004-02315/BQU and UJI-Bancaixa project P1-B2002-01 are gratefully acknowledged. This work has been supported in part by the EU under the TMR network "Exciting".

References

1. L. Bányai, S.W. Koch, *Semiconductor Quantum Dots* (Word Scientific, Singapore, 1993); L. Jacak, P. Hawrylak, A. Wójs, *Quantum Dots* (Springer, Berlin, 1998); T. Chakraborty, *Quantum dots* (Elsevier, Amsterdam, 1999)
2. D. Bimberg, M. Grundmann, N.N. Ledentsov, *Quantum Dot Heterostructures* (Wiley, Chichester, 2001)
3. A. Mews, A. Eychmüller, M. Giersig, D. Schoos, H. Weller, J. Phys. Chem. **98**, 934 (1994); X.G. Peng, L. Manna, W.D. Yang, J. Wickham, E. Scher, A. Kadavanich, A.P. Alivisatos, Nature **404**, 59 (2000); R.B. Little, M.A. El-Sayed, G.W. Bryant, S. Burke, J. Chem. Phys. **114**, 1813 (2001)
4. W. Jaskólski, G.W. Bryant, in *Optical Properties of Semiconductor Nanostructures*, edited by M.L. Sadowski, M. Potemski, M. Grynberg, NATO Science Series 3, **81** (Kluver Academic Publishers, Dordrecht, 2000); J. Planelles, J. Díaz, J. Climente, W. Jaskólski, Phys. Rev. B **65**, 245302 (2002)
5. B.C. Lee, O. Voskoboynikov, C.P. Lee, Physica E (Amsterdam) **24**, 87 (2004), and references therein
6. T. Mano, N. Koguchi, J. Crystal Growth **278**, 108 (2005)
7. Y. Masumoto, T. Takagahara, *Semiconductor Quantum Dots* (Springer, Berlin, 2002); V. Rhyzii, I. Khmyrova, V. Mitin, M. Stroscio, M. Willander, Appl. Phys. Lett. **78**, 3523 (2001); J. Phillips, J. Appl. Phys. **91**, 4590 (2002); H.C. Liu, J.Y. Duboz, R. Dudek, Z.R. Wasilewski, S. Fafard, P. Finnie, Phys. E **17**, 631 (2003)
8. T. Ihn, A. Fuhrer, L. Meier, M. Sigrist, K. Ensslin, Europhysics News **36**, 78 (2005); M. Büttiker, Y. Imry, R. Landauer, Phys. Lett. A **96**, 365 (1983); A.G. Aronov, Yu. V. Sharvin, Rev. Mod. Phys. **59**, (1987) 755; A. Fuhrer, S. Luescher, T. Ihn, T. Heinzel, K. Ensslin, W. Wegscheider, M. Bichler, Nature (London) **413**, 822 (2001)
9. Y. Aharonov, D. Bohm, Phys. Rev. **115**, 485 (1959)

10. T. Mano, T. Kuroda, S. Sanguinetti, T. Ochiai, T. Tateno, J. Kim, T. Noda, M. Kawabe, K. Sakoda, G. Kido, N. Koguchi, Nanoletters **5**, 425 (2005)
11. O. Voskoboynikov, C.P. Lee, Physica E **20**, 278 (2001)
12. S.S. Li, J.B. Xia, J. Appl. Phys. **89**, 3434 (2001)
13. J.I. Climente, J. Planelles, F. Rajadell, J. Phys: Condens. Matt. **17**, 1573 (2005)
14. B. Szafran, F.M. Peeters, Phys. Rev. B **72**, 155316 (2005)
15. G. Fuster, M. Pacheco, Z. Barticevic, Braz. J. Phys. **34**, 666 (2004)
16. J.I. Climente, J. Planelles, W. Jaskólski, Phys. Rev. B **68**, 075307 (2003)
17. A.O. Govorov, S.E. Ulloa, K. Karrai, R.J. Warburton, Phys. Rev. B **66**, R081309 (2002); see also K. Moulopoulos, M. Constantinou, Phys. Rev. B **70**, 235327 (2004)
18. K. Niemelä, P. Pietiläinen, P. Hyvönen, T. Chakraborty, Europhys. Lett. **36**, 533 (1996)